Published in final edited form as:
*Vet Pathol*. 2010 March ; 47(2): 322–333. doi:10.1177/0300985809358037.

# Morphologic and Cytokine Profile Characterization of *Salmonella enterica* Serovar Typhimurium Infection in Calves With Bovine Leukocyte Adhesion Deficiency

**J. S. Nunes**[1], **S. D. Lawhon**[1], **C. A. Rossetti**[1], **S. Khare**[1], **J. F. Figueiredo**[1], **T. Gull**[1], **R. C. Burghardt**[2], **A. J. Bäumler**[3], **R. M. Tsolis**[3], **H. L. Andrews-Polymenis**[4], and **L. G. Adams**[1]

[1] Department of Veterinary Pathobiology, College of Veterinary Medicine, Texas A&M University, College Station, Texas

[2] Department of Veterinary Integrated Biomedical Sciences, College of Medicine, Texas A&M University System Health Science Center, College Station, Texas

[4] Department of Medical Microbiology and Immunology, University of California, Davis, California

[3] Department of Medical Microbial and Molecular Pathogenesis, College of Medicine, Texas A&M University System Health Science Center, College Station, Texas

## Abstract

The role of neutrophils in the pathogenesis of *Salmonella enterica* Typhimurium–induced ruminant and human enteritis and diarrhea has yet to be characterized with in vivo models. To address this question, the in vivo bovine ligated ileal loop model of nontyphoidal salmonellosis was used in calves with the naturally occurring bovine leukocyte adhesion deficiency (BLAD) mutation whose neutrophils are unable to extravasate and infiltrate the extravascular matrix. Data obtained from 4 BLAD Holstein calves homozygous for BLAD (CD18−), 1 to 5 weeks of age, were compared to 4 controls, age-matched Holstein calves negative for BLAD (CD18+). Morphologic studies revealed that infection of CD18− calves with *S* Typhimurium resulted in no significant tissue infiltration by neutrophils, less tissue damage, reduced luminal fluid accumulation, and increased bacterial invasion, when compared to CD18+ calves. Ultrastructurally, lesions in enterocytes induced by *S* Typhimurium infection in CD18− calves—including attachment and disruption of the brush border, apical membrane ruffling formation, and cellular degeneration—were similar to the ones reported in the literature for CD18− calves. Study of cytokine gene expression by quantitative real-time polymerase chain reaction revealed that early stages of acute infection (4–8 hours postinfection) were associated with increased interleukin 8 gene expression in the absence of tissue influx of neutrophils in CD18 − calves, whereas later stages of infection (12 hours postinfection) were associated with increased expression of growth-related oncogene α in the presence of neutrophil influx in CD18+ calves. In contrast, the proinflammatory cytokines interleukin 1β and tumor necrosis factor α were poorly correlated with the presence or absence of tissue neutrophils.

Corresponding Author: Jairo S. Nunes, Covance Laboratories Inc, 671 South Meridian Road, Greenfield, IN, 46140, jairo.nunes@covance.com.

Declaration of Conflict of Interest
The authors declared that they had no conflicts of interests with respect to their authorship or the publication of this article.

**Keywords**

bovine leukocyte adhesion deficiency; cattle; chemokine; intestine; quantitative real-time polymerase chain reaction; *Salmonella enterica* Typhimurium; scanning electron microscopy; transmission electron microscopy

*Salmonella enterica* serovar Typhimurium (hereafter, *S* Typhimurium) is the most frequent animal isolate and among the three most common human isolates of nontyphoidal salmonellosis.[33] In humans, the nontyphoidal form of salmonellosis is characterized by a self-limiting enterocolitis, with diarrhea in the absence of systemic disease.[6] This form results in 200 million to 1.3 billion human cases, including 3 million deaths, each year worldwide.[38] Moreover, *S* Typhimurium is a major cause of calf morbidity and mortality, resulting in significant economic losses.[19] The 2004 *Salmonella* report published by the Centers for Disease Control and Prevenion[5] reported cattle as the most commonly identified source for *Salmonella* spp, including *S* Typhimurium, which was the most frequent serovar isolated from humans in that year. According to an analysis on the impact of foodborne illnesses, nontyphoidal salmonellosis accounts for 25.6% of hospitalizations and 30.6% of deaths owing to known foodborne pathogens in the USA.[19] The disease is markedly similar in humans and cattle, making the calf an excellent model to study the nontyphoidal form of salmonellosis.[28,40]

The morphologic changes and profile of selected chemokines, as well as proinflammatory and anti-inflammatory cytokines, have been characterized in calves by using the jejunal–ileal loop model of *S* Typhimurium–induced enteritis.[25,27] Accordingly, infection of jejunal–ileal Peyer's patches by *S* Typhimurium results in severe tissue influx of neutrophils, which is thought to play a significant role in the pathogenesis of enteritis and diarrhea induced by *S* Typhimurium infections.[25,27] The massive tissue influx of neutrophils is associated with increased expression the CXC chemokines interleukin 8 (IL-8), growth-related oncogenes α and β (GRO-α and GRO-β), and granulocyte chemotactic protein 2 (GCP-2); the proinflammatory cytokine interleukin 1β (IL-1β); and the anti-inflammatory cytokines interleukin 1Ra and interleukin 4 (IL-1Ra and IL-4).[27] In a similar study using the same model, the CXC chemokine GRO-α was considered the most important stimulus for tissue influx of neutrophils.[40] In vivo studies using the ligated intestinal loop model in rabbits found that *Salmonella*-induced fluid secretion and diarrhea are inhibited by depletion of neutrophilic pool by nitrogen mustard.[36]

Hypothetically, the tissue influx of neutrophils induces loss of epithelial integrity and effusion of a protein-rich exudate into the intestinal lumen contributing to diarrhea.[41] Alternatively, neutrophils may contribute to diarrhea by directly stimulating chloride secretion in intestinal epithelial cells. Mice experimentally infected with *S* Typhimurium typically develop the typhoid form of salmonellosis, characterized by systemic disease with a mild monocytic enteritis, minimal intestinal infiltration of neutrophils, and mild epithelial damage.[40] The classic lack of diarrhea observed in these animals corroborates the evidence that neutrophil influx plays a major role in fluid secretion. *Salmonella* effector proteins encoded by genes *sipA* (*sspA*), *sopA*, *sopB* (*sigD*), *sopD*, and *sopE2* are components of the invasion-associated type III secretion system (TTSS-1), which is required for eliciting neutrophil influx and fluid accumulation in bovine ligated ileal loops.[11,15,26,37,42] Calves infected with *S* Typhimurium, carrying simultaneous mutations in all TTSS-1-associated genes (*sipAsopABDE2* mutant or ZA21), have a markedly attenuated tissue influx of neutrophils, mild epithelial damage, and greatly reduced fluid secretion.[40,41] To develop a better understanding of the host response to nontyphoidal salmonellosis, with emphasis in the role played by neutrophils, we employed the ligated jejunal–ileal loop model in calves with bovine leukocyte adhesion deficiency (BLAD),

which is an autosomal recessive congenital condition of Holstein cattle characterized by an impaired extravasation of neutrophils into sites of inflammation.[21] The condition is caused by a single-point mutation (adenine to guanine) at position 383 of the common β2 integrin subunit CD18, resulting in defective expression of β2 integrin in the surface of leukocytes.[12,20,31] Because binding of β2 integrin expressed in the surface of activated neutrophils to intracellular adhesion molecule 1 expressed in activated endothelial cells is required for extravasation of neutrophils into sites of inflammation, the defective expression of β2 integrin in BLAD neutrophils renders these animals incapable of mounting an adequate neutrophilic response against bacterial infections.[12,21] Here, we used BLAD calves as a "neutrophil knockout" model to evaluate the histologic and ultrastructural changes and to analyze the profile of gene expression of major chemokines and proinflammatory cytokines in bovine Peyer's patches infected with *S* Typhimurium.

## Materials and Methods

### Bacterial Strains and Growth Conditions

Strains of *S* Typhimurium used in this study included the wild-type (WT) strain IR715 (ATCC 14028 WT *nal*)[32] and the mutant (MT) strain ZA21 (Δ*sipAsopABDE2* - ATCC 14028 *nal*).[42] All strains were grown in Luria–Bertani (LB) medium with nalidixic acid antibiotic (50 mg per liter) under agitation (250 revolutions per minute) overnight at 370°C; 50 μl of the culture was inoculated into 5 ml of fresh LB medium and subcultured for additional 4 hours immediately before inoculation.

### Animals, Surgical Procedure, and Sampling

These experiments used 4 BLAD Holstein calves (hereafter, CD18− calves), aged 1 to 5 weeks, represented by both sexes, and weighing approximately 35 to 55 kg. All calves were homozygous for BLAD (CD18−/−) as determined by a polymerase chain reaction–based DNA test combined with restriction enzyme analysis.[16,31] Embryo transfer[30] was used to generate 3 CD18− calves in this study. The other CD18− embryos, as well as all CD18− embryos, were donated by Drs Marcus E. Kehrli Jr and James A. Harp of the US Department of Agriculture and National Animal Disease Center, Agriculture Research Service, Ames, Iowa. The calves were kept clinically healthy before the experiments at the Large Animal Hospital of the College of Veterinary Medicine, Texas A&M University, College Station, Texas, and negative for *Salmonella* spp as determined by fecal culture using enrichment in tetrathionate broth (Difco, Detroit, MI). Calves were fed antibiotic-free milk replacer twice a day, water ad libitum, and fasted 24 hours before experimental surgeries. The ligated jejunal–ileal loop surgical procedure was employed as previously described.[27,29] Briefly, anesthesia was induced with propofol (Abbot Laboratories, Chicago, IL) followed by placement of endotracheal tube and maintenance with isofluorane (Abbot Laboratories) for the duration of the experiment. A laparotomy was performed; the ileum and jejunum were exposed; and 16 to 20 loops, 5 to 8 cm long, were ligated in the ileum and distal jejunum, intercalated with 1- to 2-cm loops. The loops were injected with 3 ml of either sterile LB broth (control, uninfected loops) or LB containing approximately $0.75 \times 10^9$ colony-forming units (cfu) of the *S* Typhimurium strains previously described. A minimum of one loop per treatment (uninfected controls, WT bacteria, or MT bacteria) per time point was infected. Infected and control loops were replaced into the abdominal cavity and excised at 1, 4, 8, and 12 hours postinfection (HPI). Samples for bacteriologic culture, histopathology, transmission and scanning electron microscopy, and quantitative real-time polymerase chain reaction (qRT-PCR) were collected. Data collected from bacteriology, fluid secretion, and gene expression of cytokines and chemokines were compared to 4 controls (hereafter, CD18+ calves)—that is, age-matched male Holstein calves negative for BLAD (CD18 +/+) submitted to similar experimental protocols.

### Fluid Secretion, Bacteriologic Culture, and Histopathology

Excised loops were opened, and the amount of accumulated fluid was measured in milliliters per loop length in centimeters (mm/cm). Two 6-mm biopsy punches were collected from the intestinal mucosa and submucosa along the antimesenteric side (including the Peyer's patches), washed three times in 5 ml of phosphate buffer saline (PBS), homogenized in 900 μl of PBS, serially diluted, and plated onto LB plates containing nalidixic acid (50 mg per liter)[42] for cfu enumeration. Intestinal samples were fixed in neutral 10% buffered formalin, processed according to routine procedures for paraffin embedding, sectioned at 4 to 5 μm, and stained with hematoxylin and eosin.

### Scanning and Transmission Electron Microscopy

Several small fragments of the intestinal samples were fixed overnight at 40°C in a solution composed of 5% glutaraldehyde and 4% paraformaldehyde in 0.1M sodium cacodylate buffer and processed as previously described.[27] Briefly, after fixation, samples were washed three times with 0.1M sodium cacodylate buffer and postfixed for 2 hours at 40°C in 1% osmium tetroxide in 0.1M sodium cacodylate buffer. For transmission electron microscopy, the samples were stained overnight at 40°C in a saturated uranyl acetate solution, dehydrated in graduated series of ethanol solutions and propylene oxide, and embedded in Epon Araldite. Sections 0.5 μm thick were stained with toluidine blue and examined under light microscopy for selection of microscopic fields that included villi, lamina propria with crypts, muscularis mucosa, and submucosa. Blocks were trimmed to produce thin sections (60 to 90 nm), mounted onto copper grids, stained with uranyl acetate and lead citrate, and examined with a Zeiss 10C transmission electron microscope. For scanning electron microscopy, samples were dehydrated, dried, coated with thin layer of AuPd (approximately 500 Å), and examined with a JEOL JSM-6400 scanning electron microscope at an accelerating voltage of 15 kV.

### Quantitative Real-Time Polymerase Chain Reaction

As a source of host RNA, eight 6-mm biopsy punches were collected from Peyer's patches. Punches were immediately cleaned to remove debris, minced into small pieces with a sterile scalpel or razor blade, immersed in 500 μl of 40°C TRI Reagent (Ambion, Foster City, CA), and further homogenized using a motorized tissue grinder. The RNA was extracted the same day according to TRI Reagent manufacturer instructions; the pellet was resuspended in nuclease-free water (Ambion); and contaminant DNA was removed by RNase-free DNase I treatment (Ambion) according to manufacturer's instructions. Samples were stored at −800° C until used. The resultant DNA-free RNA was quantified using a NanoDrop ND-1000 spectrophotometer (NanoDrop Technologies, Wilmington, DE), and assessment of RNA quality was determined using an Agilent 2100 Bioanalyser (Agilent Technologies, Santa Clara, CA).

Selected RNA samples of adequate quality from each condition were used to determine the gene expression levels of IL-8, GRO-α, IL-1β, and tumor necrosis factor α (TNF-α) by qRT-PCR, as previously described.[40] Briefly, 2 μg of RNA was reverse-transcribed at 480°C for 30 minutes with random hexamer primers and Multiscribe Reverse Transcriptase (Applied Biosystems, Foster City, CA). The resultant cDNA at a concentration of 40 ηg per sample was mixed with 4 SmartMix beads per sample (Cepheid, Sunnyvale, CA), SYBRGreen-I 0.2x (Invitrogen Corporation, Carlsbad, CA), and 500 nM of each primer set (Table 1). The qRT-PCR reaction was performed using a Smart Cycler II (Cepheid). The quantitative gene expression of each cytokine and chemokine was normalized to the internal control glyceraldehyde-3-phosphate dehydrogenase. The normalized levels of gene expression in infected tissues were calculated relative to uninfected control tissues as previously described.[40]

### Statistical Analysis

The effects of *S* Typhimurium WT and *sipAsopABDE2* MT infection on intestinal invasion, fluid secretion, and gene expression of cytokines and chemokines were analyzed by calculation of geometric means and standard deviation, followed by the use of a repeated measure analysis of variance test with Bonferroni multiple comparison adjustment to determine differences with statistical significance ($P < .05$).

## Results

### Morphologic Findings

**Histopathology—**Histologic evaluation of intestinal sections of CD18− calves was limited to the distal jejunal and ileal mucosa and submucosa. All sections from uninfected control loops were histologically within normal limits. At 1 HPI, histologic lesions in CD18− calves were not observed in tissues infected by any of the strains used (WT and MT). At this point, the absorptive villi retained normal morphology having no evidence of blunting (Fig. 1), and inflammatory infiltrates were not observed.

At 4 HPI, the first histologic changes were limited to WT-infected tissues from 3 calves characterized by mild blunting of the absorptive villi. In addition to blunting, mild exudation of fibrin into the lumen, admixed with karyorrhectic cellular debris (pseudomembrane formation), was occasionally observed, as was infrequent detachment of enterocytes from the basal membrane (Fig. 2). As with 1 HPI, inflammation was not significant in any tissues examined regardless of the infecting strain.

At 8 HPI, similar histologic lesions occurred in both WT- and MT-infected loops; however, the severity of changes was markedly reduced in tissues infected by the MT strain. In addition, significant individual animal differences in severity of lesions (regardless of the strain) were evident, with 2 calves having more severe lesions compared with the milder lesions of the remaining 2 calves. Villi were often markedly blunt, shorted, and fused (Fig. 3). Enterocytes along tips of absorptive and domed villi were occasionally detached from basement membrane and replaced or disrupted by karyorrhectic and pyknotic cellular debris, indicating necrosis, which appeared first at the tips and progressed toward the basolateral surface of villi (Fig. 4). Necrotic debris was also occasionally scattered in the lamina propria on absorptive and domed villi (Fig. 5). Inflammation was generally mild and limited to a few perivascular neutrophils in the submucosa. Neutrophils were rarely observed in the lamina propria. Occasional crypts contained a few desquamated enterocytes and necrotic debris. Crypts filled with viable and degenerate neutrophils (crypt abscesses) were not observed in any of the samples. A few mucosal and several submucosal small blood vessels (arterioles, capillaries, and venules) contained fibrin thrombi and were often packed with circulating neutrophils. Occasionally, these vessels had walls disrupted by fibrin and necrotic debris (vasculitis with fibrinoid necrosis) allowing neutrophil extravasation (Fig. 6). The submucosa was expanded by edema, fibrin, and occasional hemorrhage. A fibrinous pseudomembrane—often meager and admixed with a few desquamated enterocytes—covered the lumen in some samples.

At 12 HPI, the histologic lesions were similar in both WT- and MT-infected samples, except in the distribution of necrosis. As with 8 HPI, necrotic enterocytes tended to concentrate along the entire surface of villi in WT-infected samples, contrasting the preferential occurrence at tips of villi in MT-infected samples. The mucosa was markedly collapsed and reduced in thickness, often resulting in complete atrophy and fusion of villi. Vascular lesions similar to the ones observed at 8 HPI were more frequently seen in the submucosa. These vessels were often surrounded by large numbers of neutrophils, abundant fibrin, edema, and occasional

hemorrhage. Other lesions observed were similar to the ones described at 8 HPI for both WT- and MT-infected loops.

No histologic lesions were observed in the submucosal lymphoid tissue (Peyer's patches) in any of the samples at any time point.

**Electronmicroscopy—**Ultrastructural evaluation by transmission electron microscopy was limited to samples collected 1 HPI owing to poor preservation of ultrastructural architecture in samples from later time points. Findings were similar in WT- and MT-infected samples except for number of bacteria observed. In most sections evaluated, evidence of WT *S* Typhimurium invasion was observed in epithelial cells. In contrast, invading or internalized MT bacteria were infrequently seen. Invasion of epithelial cells was often associated with disruption of microvilli and apical membrane ruffling formation (Figs. 7, 8). Invasive bacteria commonly targeted enterocytes at tips of villi and M cells in the domed villi of the follicle-associated epithelium overlying Peyer's patches, whereas goblet cells were rarely infected. Invading organisms were located in membrane-bound vacuoles of two types: either spacious vacuoles containing multiple organisms or tight phagosomes that closely followed the contour of the bacteria. Epithelial cells containing bacteria often displayed variable degrees of degenerative changes, including cell swelling, rarefaction of cytoplasm, mitochondrial swelling with disruption of cristae, and dilation of endoplasmatic reticulum (Fig. 9). Occasional WT bacteria and rare MT bacteria were also observed within phagocytic cells in the subepithelial location in the lamina propria. Bacteria were rarely found in lymphoid follicles that compose Peyer's patches. A few infiltrating inflammatory cells within the lamina propria were occasionally observed, mostly macrophages and lymphocytes, with rare occurrence of neutrophils; the lamina propria and submucosa were often expanded by clear spaces accompanied by breakdown of collagen fibers indicating edema (Fig. 10).

Ultrastructural analysis by scanning electronmicroscopy was performed for all time points, with first changes detected in WT-infected samples at 4 HPI. Analysis of mucosal surface confirmed the presence of villi blunting, beginning at 4 HPI in WT-infected samples and 8 hours in MT-infected samples. At 12 HPI, both strains induced marked villi blunting and luminal fibrin exudation (Figs. 11, 12).

## Tissue Invasion and Fluid Secretion

Figure 13 summarizes the results of *S* Typhimurium invasion in the intestinal samples. In general, for both WT and MT bacteria, a higher number of organisms invaded the mucosa in CD18− calves as compared to CD18+ calves; however, the difference was not statistically significant at any time point. The WT strain was also found to be significantly more invasive than the MT strain in CD18+ calves at all time points. In contrast, in CD18− calves, the WT strain was significantly more invasive than the MT strain at 1 HPI only.

Quantification of the amount of fluid accumulated within the intestinal lumen for each sample demonstrated that fluid secretion in WT-infected samples was significantly reduced in CD18 − calves compared to CD18+ calves at 8 and 12 HPI (Fig. 14). Whereas CD18+ calves had significantly increased fluid secretion in WT- compared to MT-infected samples at 4 HPI and later, a significant difference between WT- and MT-infected tissues in CD18− calves was not observed at any time point (Fig. 14). Fluid accumulation was minimal in all uninfected control loops in both CD18− and CD18+ calves (data not shown).

## Chemokine and Cytokine Profile

Quantitative gene expression of major proinflammatory cytokines (IL-1β and TNF-α) and chemokines (IL-8 and GRO-α) was determined by qRT-PCR technology. IL-8 gene expression

in WT-infected samples was significantly higher in CD18− compared to CD18+ calves at 4 and 8 HPI (Fig. 15).

Gene expression of GRO-α was significantly higher in CD18+ calves compared to CD18− in WT-infected samples at 12 HPI only (Fig. 16); in addition, at this time point, GRO-α gene expression in CD18+ calves was higher in WT- compared to MT-infected samples.

Significant statistical differences in IL-1β gene expression were limited to CD18+ calves at 4 HPI, having higher expression in WT- compared to MT-infected samples. Differences in gene expression between CD18− and CD18+ calves were not observed at any time point regardless of the infected strain (Fig. 17); nevertheless, the level of IL-1β gene expression was generally higher in CD18+ than CD18− calves for most samples at most time points.

The gene expression of TNF-α, another major proinflammatory cytokine, was variable depending on the animal genotype. At 1 HPI, WT-infected samples had higher expression in CD18− compared to CD18+ calves, whereas the opposite (ie, higher expression in CD18+ than CD18−) was detected in WT-infected samples at 4 HPI (Fig. 18); in addition, MT-infected samples had higher expression in CD18− compared to CD18+ calves at 1 HPI.

## Discussion

The acute morphologic changes induced by *S* Typhimurium infection in calves, as well as the profile of cytokines and chemokines, have been well documented in previous studies using the ligated intestinal loop model.[7,13,26,27,40,42] Currently, the massive tissue influx of neutrophils is considered the histopathological hallmark of nontyphoidal salmonellosis.[35] The typical neutrophilic influx has been suggested to represent the major event triggering tissue necrosis and diarrhea.[25,27,41] Here we describe the morphologic changes induced by *S* Typhimurium infection in CD18− calves that essentially lack tissue neutrophils.

Our findings demonstrate remarkable morphologic differences in the intestine, in the absence of tissue influx of neutrophils. Whereas the first histologic lesions of villous blunting in normal calves (CD18 +/+) appeared as early as 15 minutes postinfection,[27] blunting in CD18− calves was absent at 1 HPI and first detected at 4 HPI (WT-infected samples only). Moreover, the MT strain, well known for its attenuated pathogenicity, induced the first detectable blunting at 8 HPI. In addition to blunting, detachment of epithelial cells in CD18− calves infected with the WT strain was mainly observed at 8 HPI, with only occasional occurrence at 4 hours. In contrast, this finding was commonly observed at 3 HPI[27] and first detected as early as 1 hour in CD18+ calves.[40]

Although evidence of neutrophil extravasation in CD18− calves with experimental pasteurellosis has been reported to occur in the lungs,[1–3] significant mucosal neutrophilic inflammation was not observed in any of the infected intestinal tissues. The lung, unlike other tissues, has been classically recognized as being able to recruit neutrophils through CD-18 independent pathways in studies with lung inflammatory models.[22] When present, neutrophils were limited to the perivascular connective tissue in the submucosa at 8 and 12 HPI, always associated with vascular lesions. Our data suggest that submucosal extravasation of neutrophils was caused by loss of vascular integrity secondary to vasculitis, formation of fibrin thrombi, and vascular necrosis. Vasculitis and thrombosis have been reported in CD18− calves with dermatitis.[4]

What was not observed in CD18− calves was the typical widespread necrosis of the uppermost mucosa, with complete loss of the intestinal epithelium extending to crypts reported at 8 to 12 hours in *S* Typhimurium–infected calves.[34,41] In contrast, necrosis in CD18− samples was limited to tips of villi, progressing to the basolateral surface, and a few scattered foci in the

lamina propria, presumably reflecting the pattern of bacterial invasion and dissemination. Instead of massive mucosal necrosis, the most impressive morphologic change in CD18− tissue at 12 HPI was complete atrophy and fusion of villi. This finding indicates that changes in villi morphology during nontyphoidal salmonellosis can be induced by epithelial invasion in the absence of neutrophilic inflammation.

Ultrastructurally, lesions in enterocytes induced by *S* Typhimurium infection in CD18− calves —including detachment and disruption of the brush border, apical membrane ruffling formation, and cellular degeneration—were similar to the ones reported in the literature for CD18+ calves submitted to similar experiments.[27] In addition, the published data were confirmed in our CD18− samples, identifying cell tropism of *S* Typhimurium for M cells in the follicle-associated epithelium of Peyer's patches and epithelial cells at the tips of absorptive villi.[10,27]

The most remarkable and surprising morphologic difference between the typical lesions of *S* Typhimurium–induced enteritis in normal calves compared to CD18− calves in this study was the complete absence of lesions in Peyer's patches. Acute salmonellosis in calves is typically associated with lymphocyte depletion in Peyer's patches follicles,[27] progressing to necrosis in chronic stages of infection.[39] The absence of significant lesions in CD18− calves suggests that necrosis of Peyer's patches in salmonellosis occurs as a consequence of neutrophilic infiltration within lymphoid follicles, as opposed to the bacterial infection of cells and their transport into the lymphoid follicles. This hypothesis is supported by evidence that neutrophilic infiltration in Peyer's patches–infected samples precedes lymphoid depletion and necrosis in calves.[27]

Invasion of *S* Typhimurium in bovine ligated jejunal–ileal loops is dependent on the synergistic effects of TTSS-1-encoded effector proteins sipA, sopA, sopB, sopD, sopE, and sopE2.[23,42] In this study, mucosal invasion of *Salmonella* was generally increased in CD18− compared to CD18+ calves, though not statistically significant at any time point. In addition, for most time points (4 to 12 HPI), we observed that the MT strain was not found to be significantly less invasive than the WT strain in CD18− calves. This finding was opposed to the lower invasiveness of MT compared to WT bacteria as confirmed by our data on CD18+ calves and as reported in the literature.[40,41] Collectively, these data suggest that tissue influx of neutrophils partially reduces mucosal invasion of WT *S* Typhimurium and largely contributes to preventing the invasion of the MT strain. The mechanism responsible for fluid secretion and diarrhea in nontyphoidal models of salmonellosis remains to be elucidated. Studies in bovine ligated ileal loops strongly support an exudative mechanism, rather than secretory diarrhea (chloride secretion), as the most likely mechanism.[41] Accordingly, the massive intestinal influx of neutrophils in calves infected with *S* Typhimurium results in necrosis with loss of epithelial integrity and diarrhea by an exudative mechanism.[41] Our data provide strong evidence that fluid accumulation in CD18− calves is significantly reduced compared to CD18+ calves at later time points when inflammation is normally most severe (ie, at 8 and 12 HPI). As with bacterial invasion, the markedly different degree of responses between WT- and MT-infected samples observed in CD18+ calves was less evident in CD18− calves, supporting the hypothesis that the neutrophilic influx plays a crucial role in the pathogenesis of both strains, especially preventing pathologic effects caused by the MT strain. Our findings support the hypothesis of exudative diarrhea secondary to inflammation as the major contributor to the fluid secretion in nontyphoidal salmonellosis. However, it is important to realize that, though markedly reduced, fluid secretion in CD18− calves still occurred. It is yet to be determined if the mild fluid accumulation observed in CD18− calves resulted from either secretory mechanisms secondary to the necrosis and vascular lesions or a combination thereof as commonly observed at 8 and 12 hours postinfection.

The type of inflammatory infiltrate that characterizes a disease is controlled in part by the profile of inflammatory cytokines and chemokines.[18] The proinflammatory cytokines IL-1β and TNF-α, as well as potent neutrophil chemoattractants, the CXC chemokines IL-8 and GRO-α, have been suggested to play major roles during *S* Typhimurium–induced enteritis and diarrhea in calves.[25,27,41] Besides being often expressed in the bovine model of nontyphoidal salmonellosis, IL-8 gene expression is induced in human epithelial cell lines by the *S* Typhimurium TTSS-1.[14] We found that gene expression of IL-8 in WT-infected samples was significantly higher in CD18− than in CD18+ calves at 4 and 8 HPI. A possible interpretation of this finding is that the absence of tissue neutrophils in CD18− triggers a positive feedback mechanism for production of more IL-8 via unknown pathways in an attempt to recruit neutrophils necessary to control infection. This finding also suggests that neutrophils are unlikely to be the major source of IL-8 during *S* Typhimurium infection in calves given that increased gene expression in CD18− occurred in the absence of significant tissue influx of neutrophils. Studies using the bovine ligated ileal loop model have identified the GRO-α chemokine as the major chemoattractant for neutrophils during *S* Typhimurium–induced enteritis.[40] Our data on GRO-α gene expression in CD18+ calves confirmed the high expression levels—up to an 80-fold increase over uninfected control in WT-infected samples, especially in the later stages of acute infection (ie, at 12 HPI). This finding suggests that the massive influx of neutrophils observed in the later phase of acute infection is mainly driven by GRO-α. In CD18− calves, however, the GRO-α gene expression at WT-infected samples at this late stage of infection was significantly reduced compared to CD18+, indicating that the neutrophil influx may play a role in triggering GRO-α gene expression in the later phase of acute infection by either directly secreting this chemokine or stimulating its production in other cell types indirectly. IL-1β and TNF-α are classic proinflammatory cytokines increased during *Salmonella* infection in all organs studied to date using in vivo models of infection.[8,17,27] Extensive evidence from studies in mice indicates that these cytokines are essential for host defense against *Salmonella* infection.[9] In bovine ligated ileal loops infected with *S* Typhimurium, the gene expression of these two cytokines was determined by conventional reverse transcription polymerase chain reaction. Accordingly, the expression of IL-1β was elevated at 3 and 6 HPI, whereas no changes in gene expression was detected for TNF-α after infection.[24] Although not statistically significant, our data confirmed that the gene expression levels of IL-1β in CD18− calves were lower than those of CD18+ calves, especially in WT-infected samples ($P = .109$ at 8 HPI). These data were expected in view of the essentially absent tissue inflammation in the CD18− calves. The lack of statistical significance in the different expression levels of IL-1β between CD18− and CD18+ calves could be explained by the high standard deviation observed in our data as a result of marked individual variability. More experimental samples are necessary to increase the statistical power and confirm our findings regarding IL-1β gene expression. The TNF-α gene expression in our CD18− samples was variable in WT-infected samples, with significantly higher expression in CD18− at 1 HPI, but with the opposite relationship (ie, higher expression) occurring in CD18+ calves at 4 HPI. These results, combined with our finding of no significant differences in TNF-α gene expression between CD18− and CD18+ calves at later time points, suggest that neutrophil influx likely plays a minor role in the gene expression of this cytokine during *S* Typhimurium–induced enteritis in calves.

In conclusion, infection by *S* Typhimurium of ligated ileal loops in calves with BLAD resulted in markedly distinct morphologic changes as well as chemokine and cytokine profiles, compared to normal animals negative for BLAD. The most important differences essentially included the absence of typical *S* Typhimurium–induced neutrophilic enteritis, the unique pattern and reduced magnitude of necrosis, and the differential gene expression profiles of major neutrophil chemokines and proinflammatory cytokines. The differences in CD18− calves were associated with a significantly increased bacterial invasion and reduced fluid accumulation, supporting the hypothesis that *S* Typhimurium–induced diarrhea in normal

calves is primarily exudative and caused by the massive tissue influx of neutrophils. New evidence provided by these experiments significantly extends our understanding of the morphologic and molecular pathogenesis of diarrhea of human and ruminant nontyphoidal salmonellosis.

## Acknowledgments

We thank Soma Dhavala for his extensive and valuable contributions to the statistical analysis. We also thank Roberta Pugh and Doris Hunter for their technical assistance throughout the experiment, in addition to Alan Patranella and Linda McCallum for their assistance with the experimental surgeries. Expert technical assistance with scanning and transmission electron micrographs was provided by Drs Helga Sittertz-Bhatkar and Ross Payne. Finally, we thank Rosemary Vollmar and the staff of the histology laboratory in the Veterinary Pathobiology Department at Texas A&M University for their assistance with the histologic sections. Funding was provided by grants to A.J.B. and L.G.A. from the National Institutes of Health (1 RO1 A144170-01A1) and the US Department of Agriculture, Cooperative State Research, Education, and Extension Service (National Research Initiative 2002-35204-12247).

Financial Disclosure/Funding

Funding was provided by grants to A.J.B. and L.G.A. from the National Institutes of Health (1 RO1 A144170-01A1) and the US Department of Agriculture, Cooperative State Research, Education, and Extension Service (National Research Initiative 2002-35204-12247).

## References

1. Ackermann MR, Brogden KA, Florance AF, Kehrli ME Jr. Induction of CD18− mediated passage of neutrophils by *Pasteurella haemolytica* in pulmonary bronchi and bronchioles. Infect Immun 1999;67:659–663. [PubMed: 9916073]
2. Ackermann MR, Kehrli ME Jr, Brogden KA. Passage of CD18− and CD18+ bovine neutrophils into pulmonary alveoli during acute *Pasteurella haemolytica* pneumonia. Vet Pathol 1996;33:639–646. [PubMed: 8952022]
3. Ackermann MR, Kehrli ME Jr, Laufer JA, Nusz LT. Alimentary and respiratory tract lesions in eight medically fragile Holstein cattle with bovine leukocyte adhesion deficiency (BLAD). Vet Pathol 1996;33:273–281. [PubMed: 8740700]
4. Ackermann MR, Kehrli ME Jr, Morfitt DC. Ventral dermatitis and vasculitis in a calf with bovine leukocyte adhesion deficiency. J Am Vet Med Assoc 1993;202:413–415. [PubMed: 8440633]
5. Centers for Disease Control and Prevention. Salmonella Surveillance: Annual Summary, 2004. US Department of Health and Human Services; Atlanta, GA: 2005.
6. Coburn B, Grassl GA, Finlay BB. *Salmonella*, the host and disease: a brief review. Immunol Cell Biol 2007;85:112–118. [PubMed: 17146467]
7. Coombes BK, Coburn BA, Potter AA, Gomis S, Mirakhur K, Li Y, Finlay BB. Analysis of the contribution of *Salmonella* pathogenicity islands 1 and 2 to enteric disease progression using a novel bovine ileal loop model and a murine model of infectious enterocolitis. Infect Immun 2005;73:7161–7169. [PubMed: 16239510]
8. Eckmann L, Fierer J, Kagnoff MF. Genetically resistant (Ityr) and susceptible (Itys) congenic mouse strains show similar cytokine responses following infection with *Salmonella dublin*. J Immunol 1996;156:2894–2900. [PubMed: 8609409]
9. Eckmann L, Kagnoff MF. Cytokines in host defense against *Salmonella*. Microbes Infect 2001;3:1191–1200. [PubMed: 11755407]
10. Frost AJ, Bland AP, Wallis TS. The early dynamic response of the calf ileal epithelium to *Salmonella typhimurium*. Vet Pathol 1997;34:369–386. [PubMed: 9381648]
11. Galyov EE, Wood MW, Rosqvist R, Mullan PB, Watson PR, Hedges S, Wallis TS. A secreted effector protein of *Salmonella dublin* is translocated into eukaryotic cells and mediates inflammation and fluid secretion in infected ileal mucosa. Mol Microbiol 1997;25:903–912. [PubMed: 9364916]
12. Gerardi AS. Bovine leukocyte adhesion deficiency: a brief overview of a modern disease and its implications. Acta Vet Hung 1996;44:1–8. [PubMed: 8826696]

13. Haque A, Bowe F, Fitzhenry RJ, Frankel G, Thomson M, Heuschkel R, Murch S, Stevens MP, Wallis TS, Phillips AD, Dougan G. Early interactions of *Salmonella enterica* serovar typhimurium with human small intestinal epithelial explants. Gut 2004;53:1424–1430. [PubMed: 15361488]

14. Hobbie S, Chen LM, Davis RJ, Galan JE. Involvement of mitogen-activated protein kinase pathways in the nuclear responses and cytokine production induced by *Salmonella typhimurium* in cultured intestinal epithelial cells. J Immunol 1997;159:5550–5559. [PubMed: 9548496]

15. Jones MA, Wood MW, Mullan PB, Watson PR, Wallis TS, Galyov EE. Secreted effector proteins of *Salmonella dublin* act in concert to induce enteritis. Infect Immun 1998;66:5799–5804. [PubMed: 9826357]

16. Kehrli ME Jr, Schmalstieg FC, Anderson DC, Van der Maaten MJ, Hughes BJ, Ackermann MR, Wilhelmsen CL, Brown GB, Stevens MG, Whetstone CA. Molecular definition of the bovine granulocytopathy syndrome: identification of deficiency of the Mac-1 (CD11b/CD18) glycoprotein. Am J Vet Res 1990;51:1826–1836. [PubMed: 1978618]

17. Klimpel GR, Asuncion M, Haithcoat J, Niesel DW. Cholera toxin and *Salmonella typhimurium* induce different cytokine profiles in the gastrointestinal tract. Infect Immun 1995;63:1134–1137. [PubMed: 7868239]

18. Luster AD. Chemokines—chemotactic cytokines that mediate inflammation. N Engl J Med 1998;338:436–445. [PubMed: 9459648]

19. Mead PS, Slutsker L, Dietz V, McCaig LF, Bresee JS, Shapiro C, Griffin PM, Tauxe RV. Food-related illness and death in the United States. Emerg Infect Dis 1999;5:607–625. [PubMed: 10511517]

20. Nagahata H. Bovine leukocyte adhesion deficiency (BLAD): a review. J Vet Med Sci 2004;66:1475–1482. [PubMed: 15644595]

21. Nagahata H, Kehrli ME Jr, Murata H, Okada H, Noda H, Kociba GJ. Neutrophil function and pathologic findings in Holstein calves with leukocyte adhesion deficiency. Am J Vet Res 1994;55:40–48. [PubMed: 7908182]

22. Petri B, Phillipson M, Kubes P. The physiology of leukocyte recruitment: an in vivo perspective. J Immunol 2008;180:6439–6446. [PubMed: 18453558]

23. Raffatellu, M.; Tukel, C.; Chessa, D.; Wilson, RP.; Baumler, AJ. The intestinal phase of *Salmonella* infections. In: Rhen, M.; Maskell, M.; Mastroeni, P.; Threlfall, J., editors. Salmonella Mollecular Biology and Pathogenesis. Norfolk; UK: 2007. p. 31-51.

24. Santos RL, Schoffelmeer JA, Tsolis RM, Gutierrez-Pabello JA, Baumler AJ, Adams LG. *Salmonella* serotype Typhimurium infection of bovine Peyer's patches down-regulates plasma membrane calcium-transporting ATPase expression. J Infect Dis 2002;186:372–378. [PubMed: 12134233]

25. Santos RL, Tsolis RM, Baumler AJ, Adams LG. Pathogenesis of *Salmonella*-induced enteritis. Braz J Med Biol Res 2003;36:3–12. [PubMed: 12532221]

26. Santos RL, Tsolis RM, Zhang S, Ficht TA, Baumler AJ, Adams LG. *Salmonella*-induced cell death is not required for enteritis in calves. Infect Immun 2001;69:4610–4617. [PubMed: 11402005]

27. Santos RL, Zhang S, Tsolis RM, Baumler AJ, Adams LG. Morphologic and molecular characterization of *Salmonella typhimurium* infection in neonatal calves. Vet Pathol 2002;39:200–215. [PubMed: 12009058]

28. Santos RL, Zhang S, Tsolis RM, Kingsley RA, Adams LG, Baumler AJ. Animal models of *Salmonella* infections: enteritis versus typhoid fever. Microbes Infect 2001;3:1335–1344. [PubMed: 11755423]

29. Schesser K, Dukuzumuremyi JM, Cilio C, Borg S, Wallis TS, Pettersson S, Galyov EE. The *Salmonella* YopJ-homologue AvrA does not possess YopJ-like activity. Microb Pathog 2000;28:59–70. [PubMed: 10644492]

30. Seidel GE Jr. Superovulation and embryo transfer in cattle. Science 1981;211:351–358. [PubMed: 7194504]

31. Shuster DE, Kehrli ME Jr, Ackermann MR, Gilbert RO. Identification and prevalence of a genetic defect that causes leukocyte adhesion deficiency in Holstein cattle. Proc Natl Acad Sci U S A 1992;89:9225–9229. [PubMed: 1384046]

32. Stojiljkovic I, Baumler AJ, Heffron F. Ethanolamine utilization in *Salmonella typhimurium*: nucleotide sequence, protein expression, and mutational analysis of the cchA cchB eutE eutJ eutG eutH gene cluster. J Bacteriol 1995;177:1357–1366. [PubMed: 7868611]
33. Swaminathan B, Gerner-Smidt P, Barrett T. Focus on *Salmonella*. Foodborne Pathog Dis 2006;3:154–156. [PubMed: 16761940]
34. Tsolis RM, Adams LG, Ficht TA, Baumler AJ. Contribution of *Salmonella typhimurium* virulence factors to diarrheal disease in calves. Infect Immun 1999;67:4879–4885. [PubMed: 10456944]
35. Tukel C, Raffatellu M, Chessa D, Wilson RP, Akcelik M, Baumler AJ. Neutrophil influx during non-typhoidal salmonellosis: who is in the driver's seat? FEMS Immunol Med Microbiol 2006;46:320–329. [PubMed: 16553804]
36. Wallis TS, Vaughan AT, Clarke GJ, Qi GM, Worton KJ, Candy DC, Osborne MP, Stephen J. The role of leucocytes in the induction of fluid secretion by *Salmonella typhimurium*. J Med Microbiol 1990;31:27–35. [PubMed: 2404124]
37. Wood MW, Jones MA, Watson PR, Siber AM, McCormick BA, Hedges S, Rosqvist R, Wallis TS, Galyov EE. The secreted effector protein of *Salmonella dublin*, SopA, is translocated into eukaryotic cells and influences the induction of enteritis. Cell Microbiol 2000;2:293–303. [PubMed: 11207586]
38. World Health Organization. Drug-Resistant Salmonella. [Accessed December 3, 2009]. http://www.who.int/mediacentre/factsheets/fs139/en/. Published April 2005
39. Wray C, Sojka WJ. Experimental *Salmonella typhimurium* infection in calves. Res Vet Sci 1978;25:139–143. [PubMed: 364573]
40. Zhang S, Adams LG, Nunes J, Khare S, Tsolis RM, Baumler AJ. Secreted effector proteins of *Salmonella enterica* serotype typhimurium elicit host-specific chemokine profiles in animal models of typhoid fever and enterocolitis. Infect Immun 2003;71:4795–4803. [PubMed: 12874363]
41. Zhang S, Kingsley RA, Santos RL, Andrews-Polymenis H, Raffatellu M, Figueiredo J, Nunes J, Tsolis RM, Adams LG, Baumler AJ. Molecular pathogenesis of *Salmonella enterica* serotype typhimurium-induced diarrhea. Infect Immun 2003;71:1–12. [PubMed: 12496143]
42. Zhang S, Santos RL, Tsolis RM, Stender S, Hardt WD, Baumler AJ, Adams LG. The *Salmonella enterica* serotype typhimurium effector proteins SipA, SopA, SopB, SopD, and SopE2 act in concert to induce diarrhea in calves. Infect Immun 2002;70:3843–3855. [PubMed: 12065528]

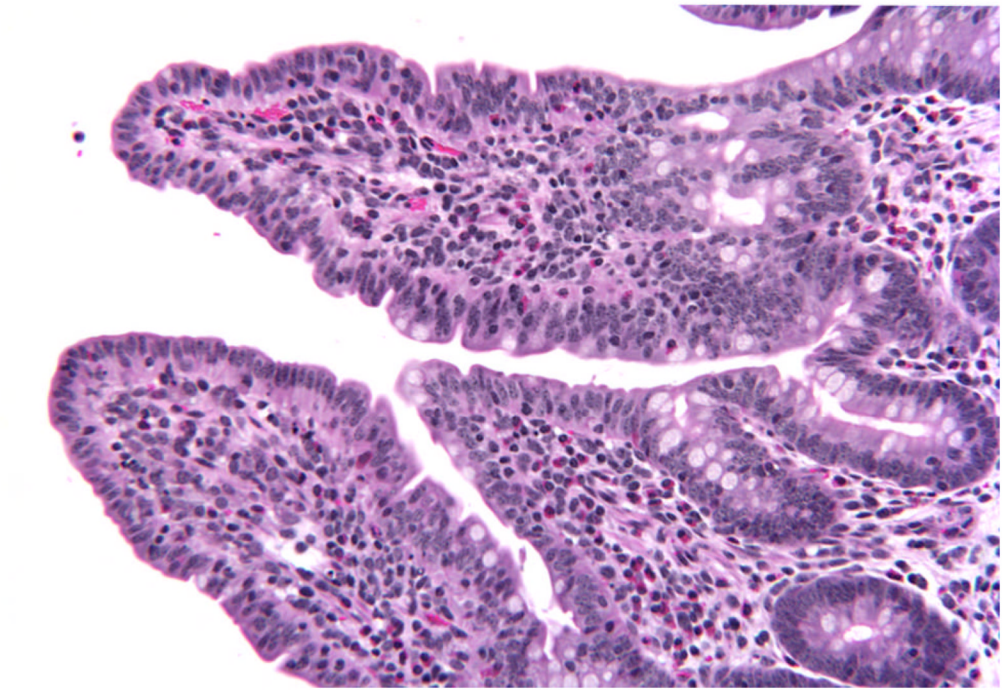

**Figure 1.**
Ileum; CD18− calf, wild-type-infected sample. Normal histologic appearance of absorptive villi at 1 hour postinfection. HE. CD18−, bovine leukocyte adhesion deficiency.

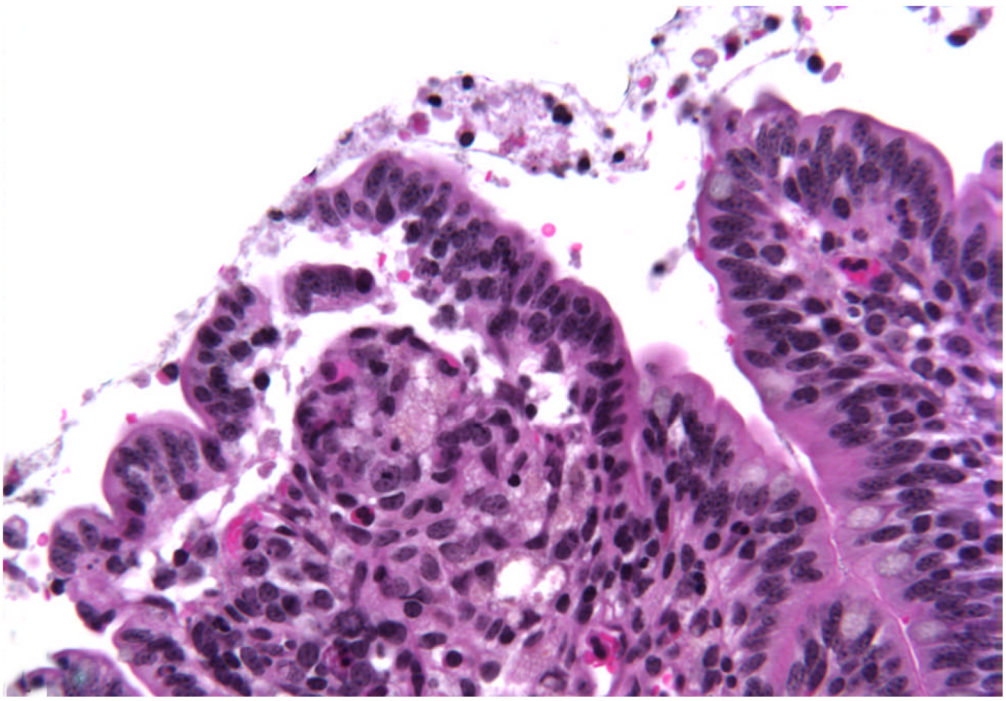

**Figure 2.**
Ileum; CD18− calf, wild-type-infected sample. Detachment of enterocytes at tip of absorptive villi with fibrinous pseudomembrane formation at 4 hours postinfection. HE stain. CD18−, bovine leukocyte adhesion deficiency.

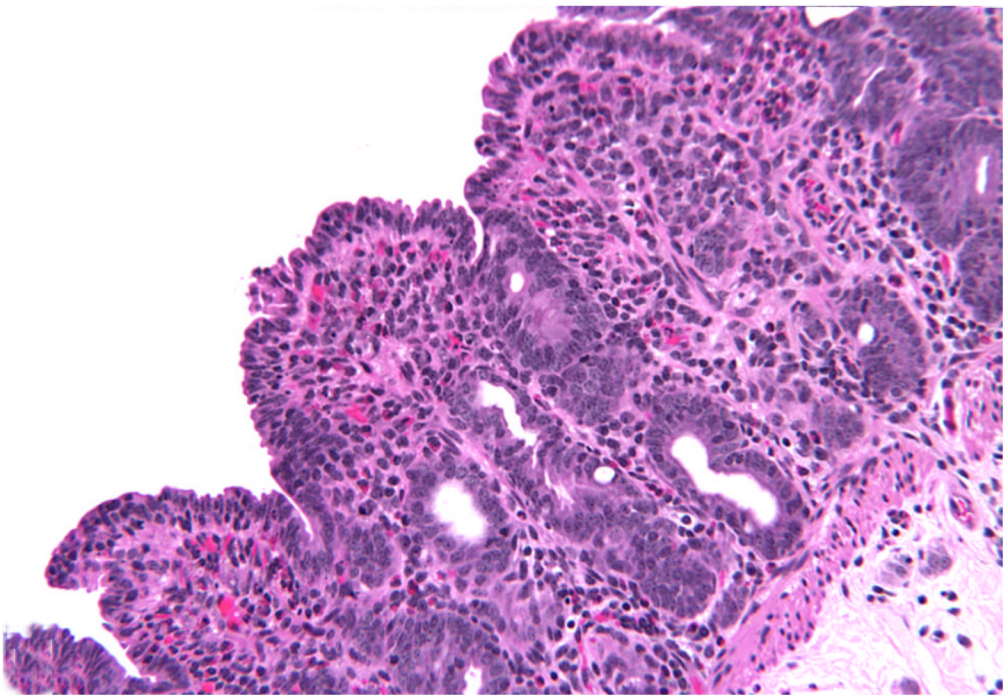

**Figure 3.**
Ileum; CD18− calf, wild-type-infected sample. Marked blunting, shortening, and fusion of villi at 8 hours postinfection. HE. CD18−, bovine leukocyte adhesion deficiency.

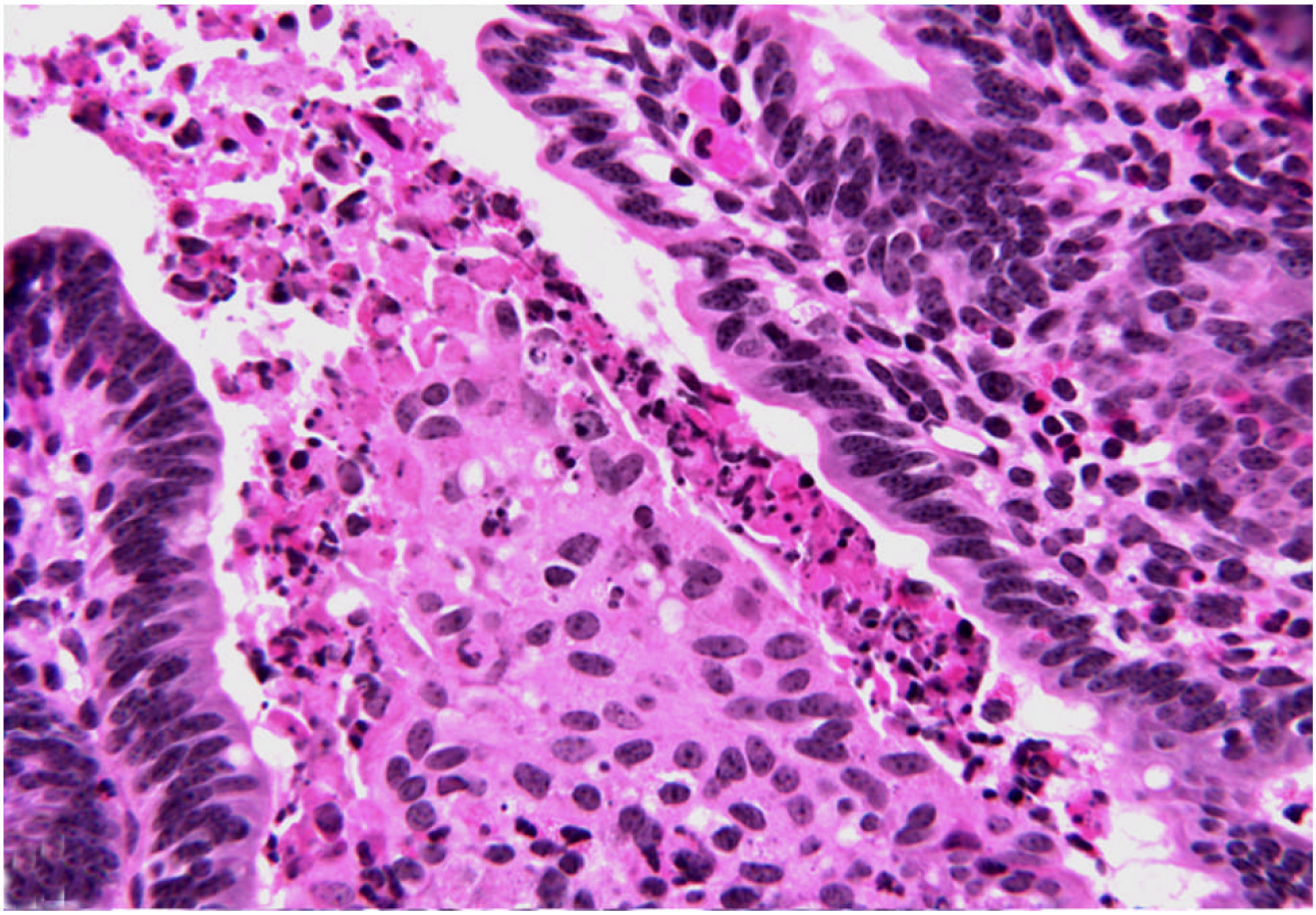

**Figure 4.**
Ileum; CD18− calf, wild-type-infected sample. Necrosis at villous tips and basolateral surface at 8 hours postinfection. HE. CD18−, bovine leukocyte adhesion deficiency.

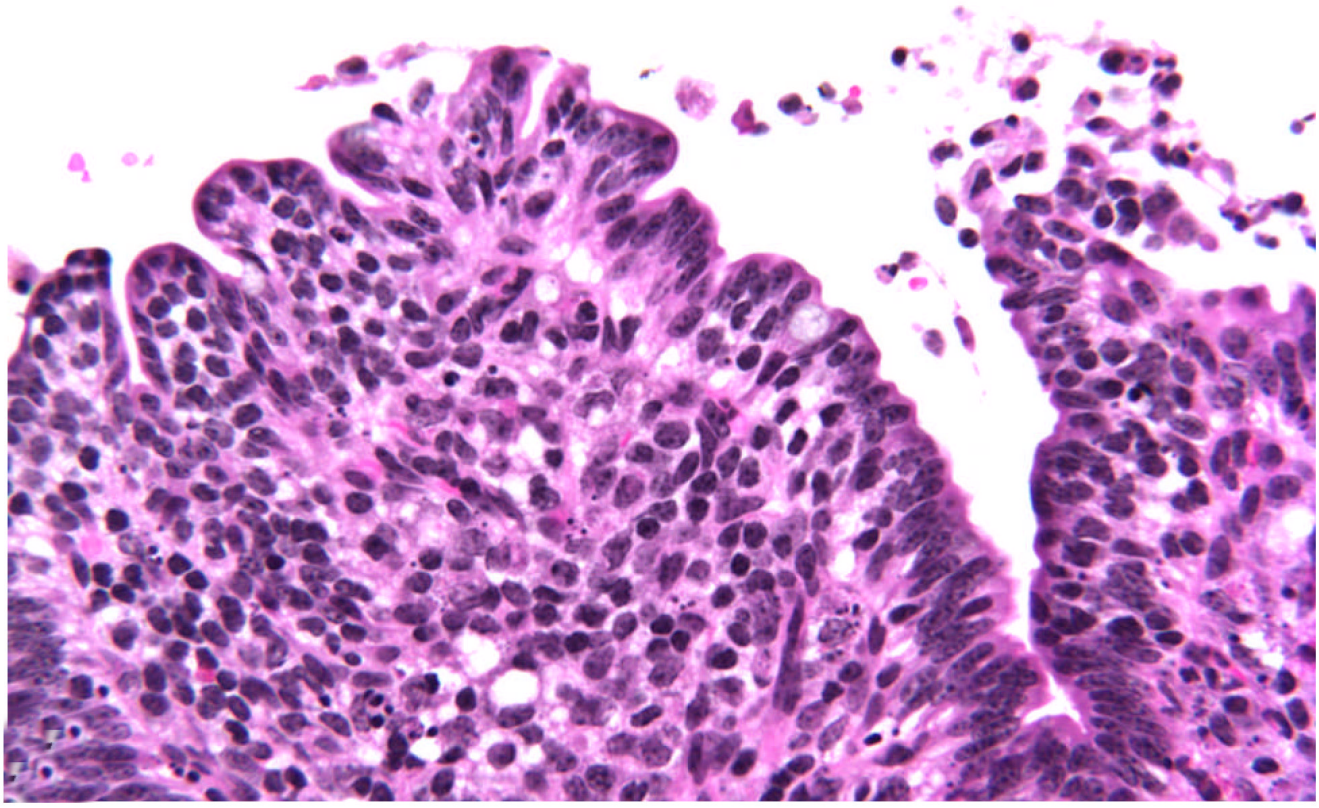

**Figure 5.**
Ileum; CD18− calf, wild-type-infected sample. Scattered necrosis throughout the lamina propria of villi at 8 hours postinfection. HE. CD18−, bovine leukocyte adhesion deficiency.

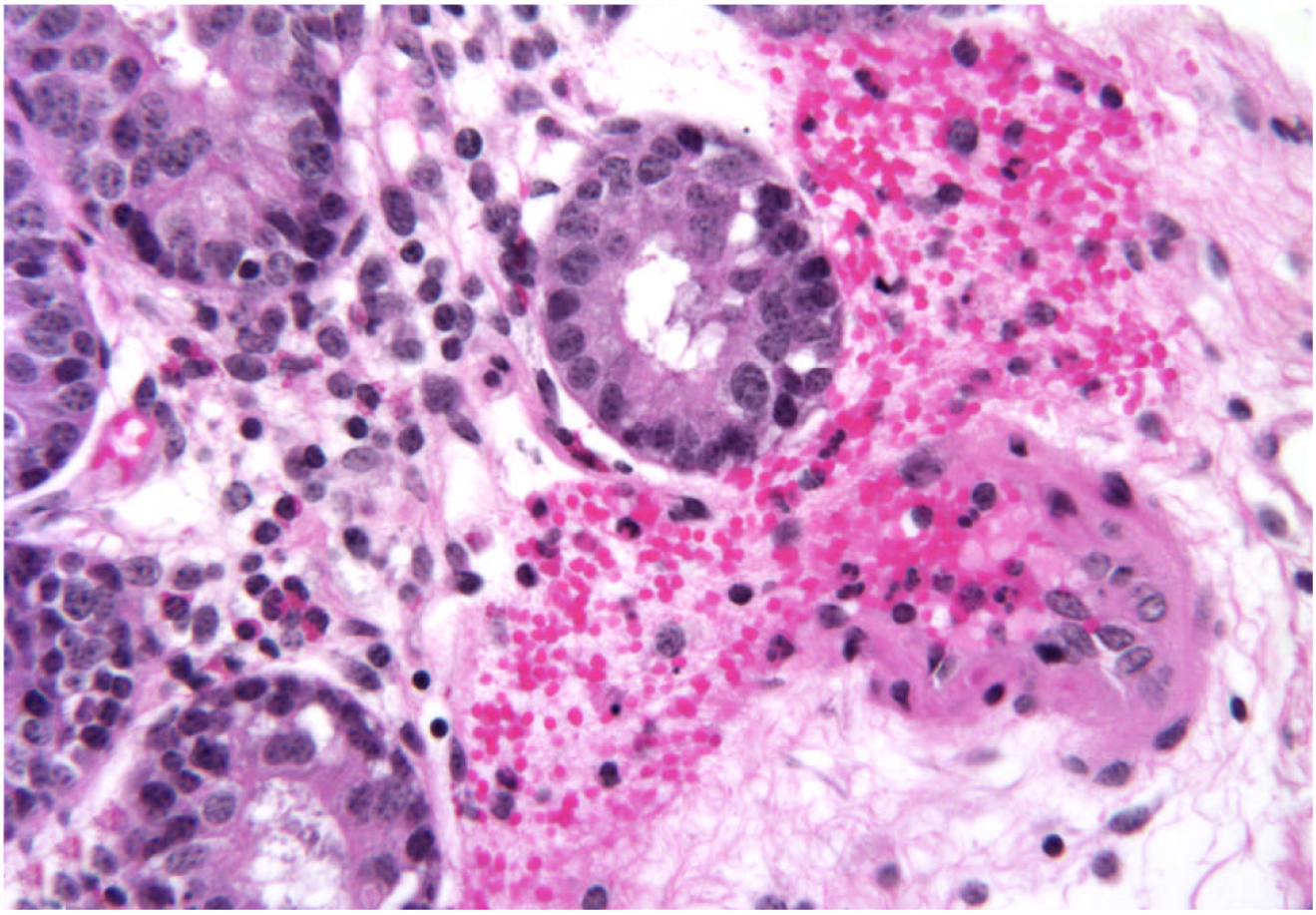

**Figure 6.**
Ileum; CD18− calf, wild-type-infected sample. Vascular necrosis with extravasation of neutrophils and erythrocytes into the submucosa at 8 hours postinfection. HE. CD18−, bovine leukocyte adhesion deficiency.

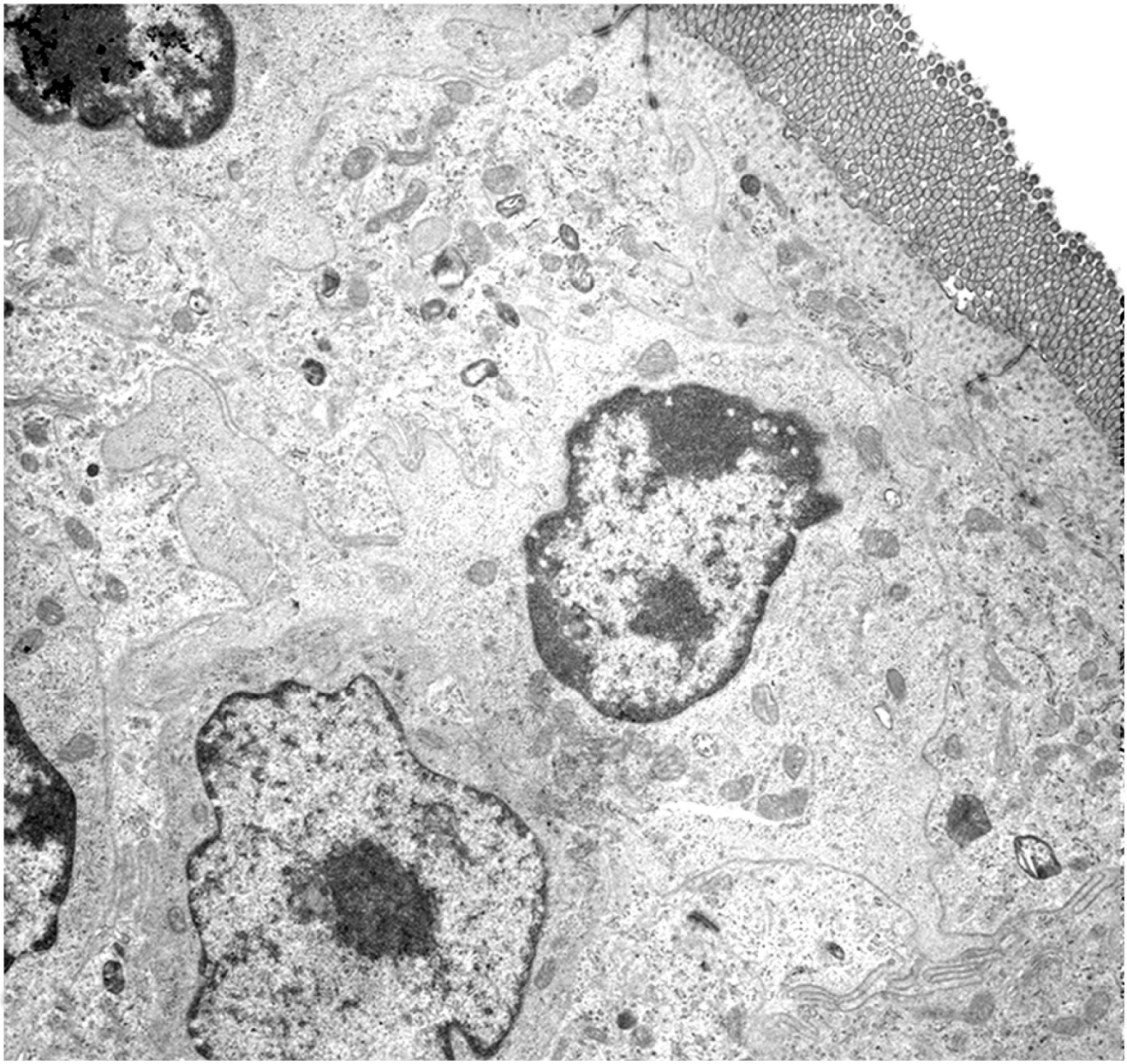

**Figure 7.**
Transmission electron micrograph. Ileum; CD18− calf, uninfected control. Normal enterocytes in the tip of villi at 1 hour postinfection. CD18−, bovine leukocyte adhesion deficiency.

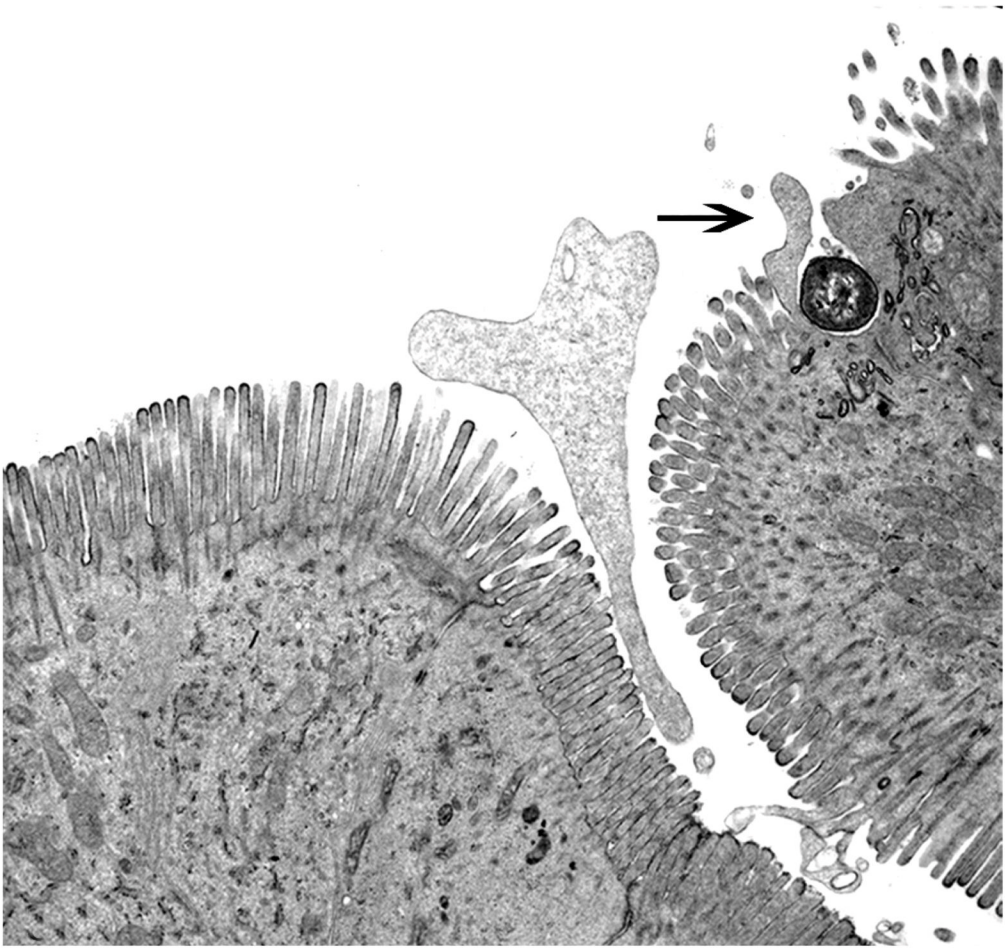

**Figure 8.**
Transmission electron micrograph. Ileum; CD18− calf, wild-type-infected sample. *Salmonella* Typhimurium–induced disruption of the brush border and membrane ruffling (arrow) at 1 hour postinfection. CD18−, bovine leukocyte adhesion deficiency.

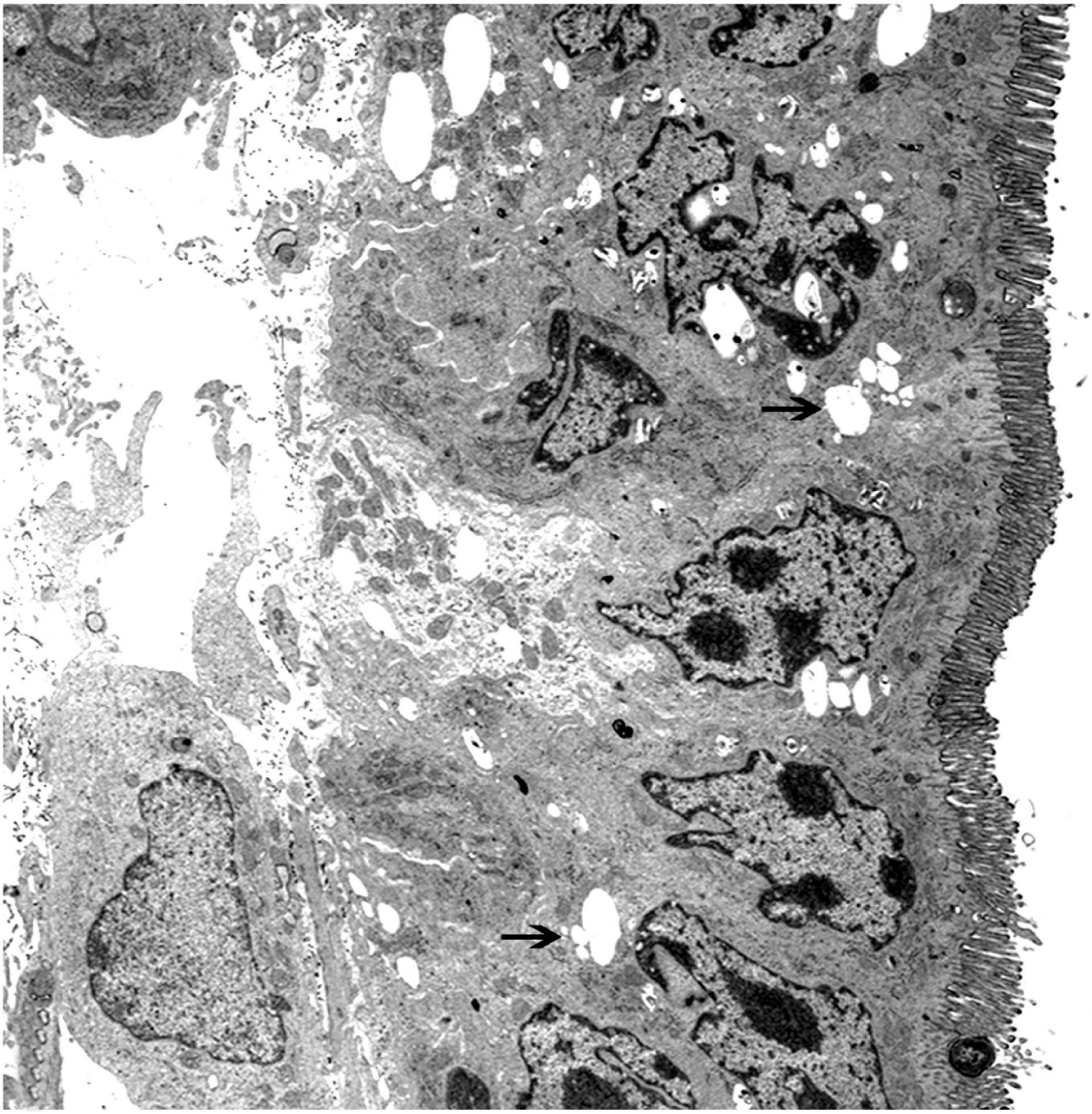

**Figure 9.**
Transmission electron micrograph. Ileum; CD18− calf, wild-type-infected sample. Infected cells showing evidence of degeneration, including cytoplasmic swelling, rarefaction, loss of organelles, and dilation of endoplasmatic reticulum (arrows) at 1 hour postinfection. CD18−, bovine leukocyte adhesion deficiency.

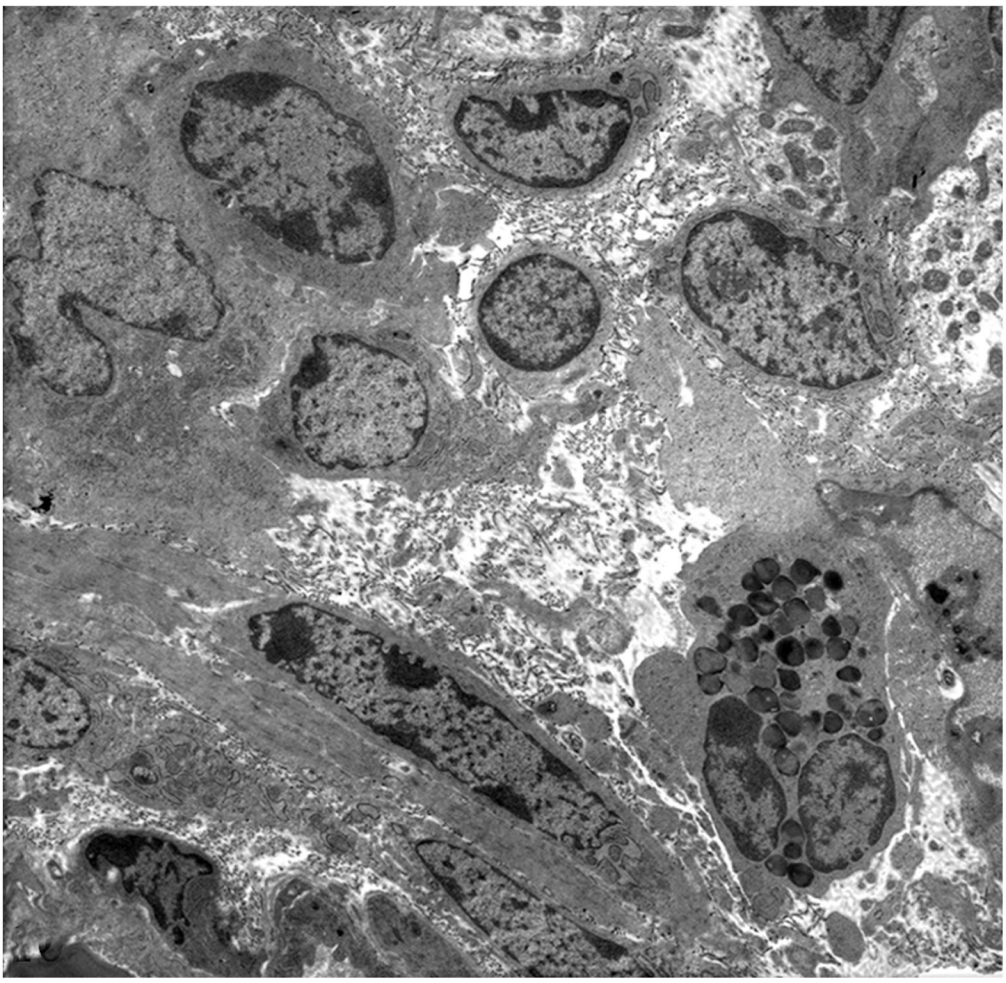

**Figure 10.**
Transmission electron micrograph. Ileum; CD18− calf, wild-type-infected sample. Infected lamina propria showing clear spaces with breakdown of collagen fibers (edema) and rare neutrophils at 1 hour postinfection. CD18−, bovine leukocyte adhesion deficiency.

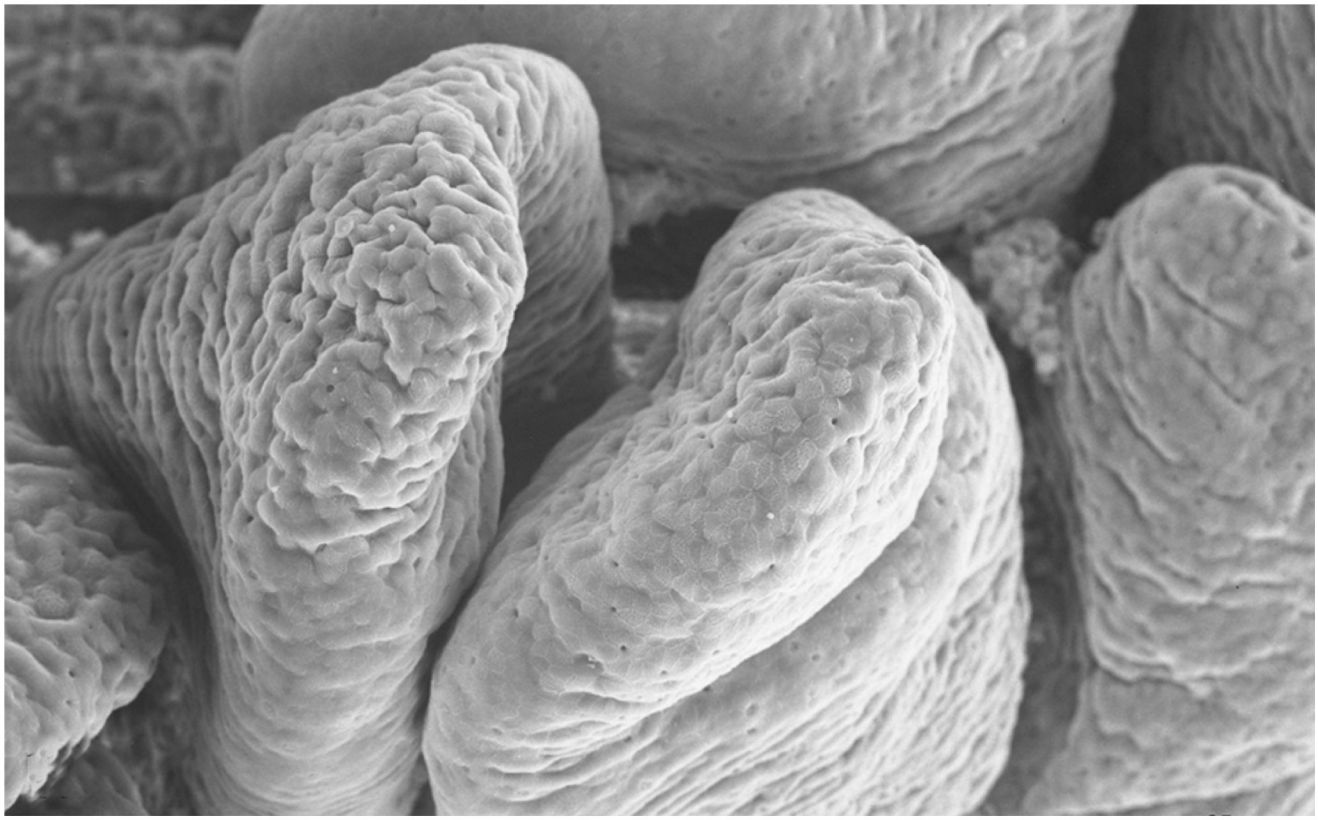

**Figure 11.**
Scanning electron micrograph. Ileum; CD18− calf, uninfected control. Normal appearance of villi at 1 hour postinfection. CD18−, bovine leukocyte adhesion deficiency.

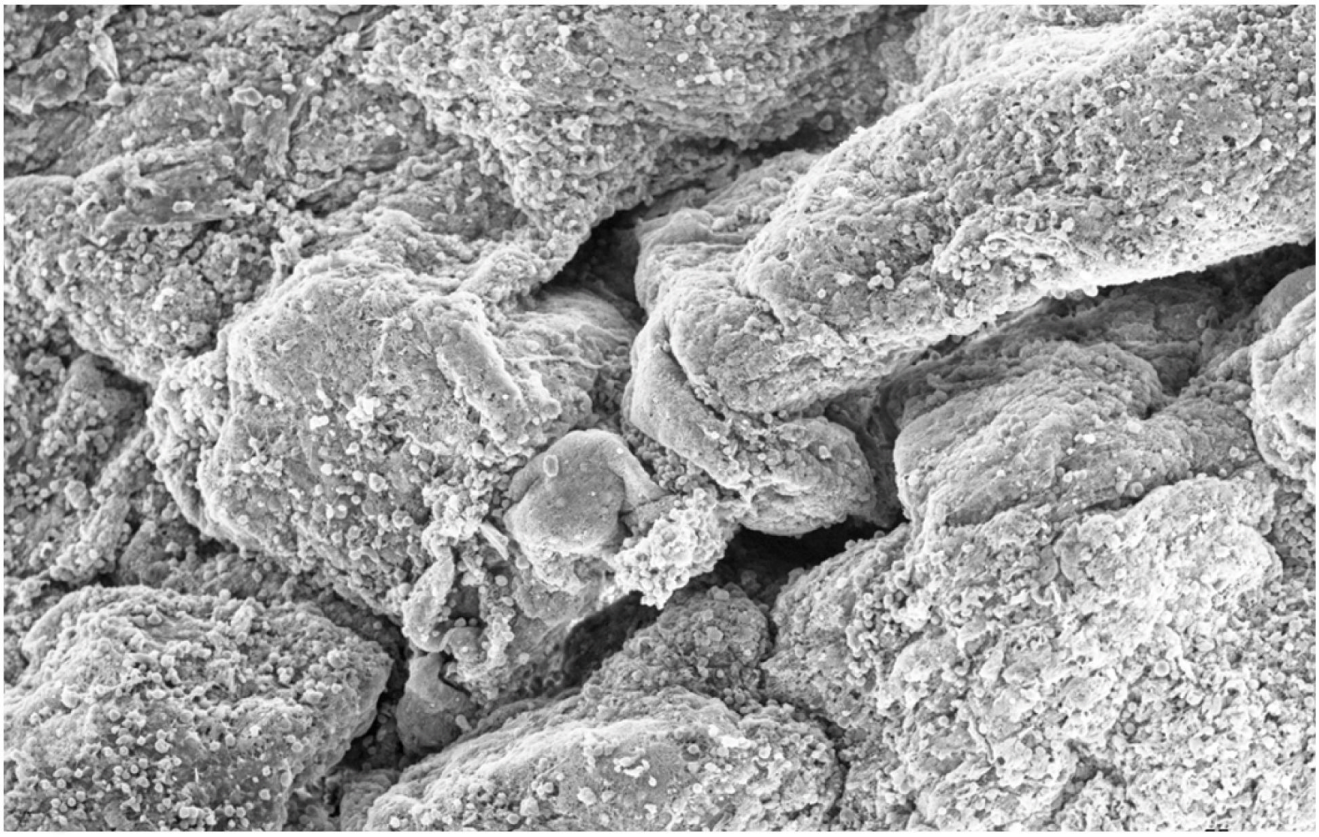

**Figure 12.**
Scanning electron micrograph. Ileum; CD18− calf, wild-type-infected sample. Severe villous atrophy and luminal fibrin exudation (pseudomembrane formation) at 12 hours postinfection. CD18−, bovine leukocyte adhesion deficiency.

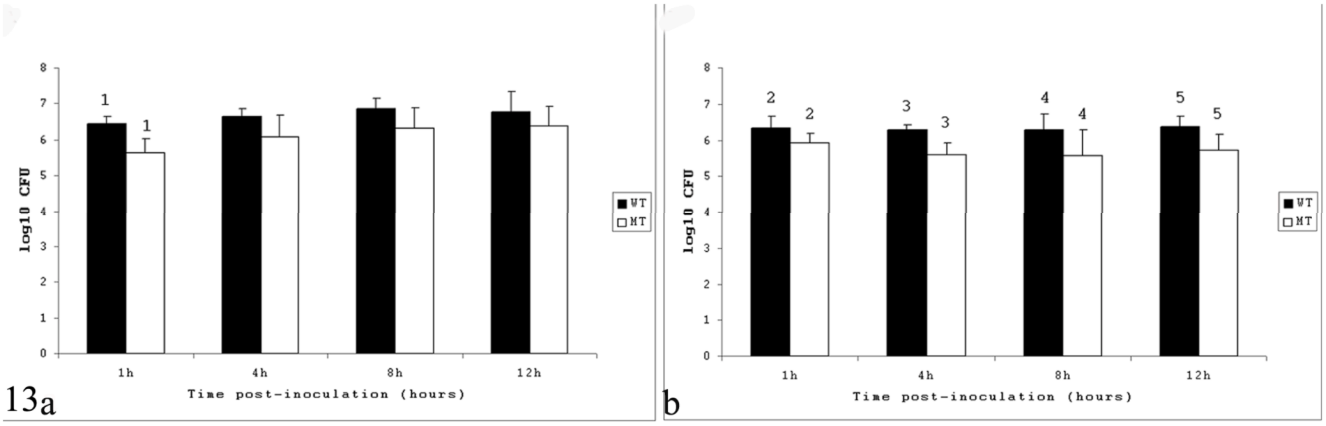


**Figure 13.**
Mucosal invasion of wild-type (WT) or mutant (MT) *Salmonella* Typhimurium in CD18− (A) and CD18+ (B) calves at 1, 4, 8, and 12 hours postinfection. Conditions labeled with the same number are statistically different ($P < .05$). CD18−, bovine leukocyte adhesion deficiency; CD18+, no deficiency.

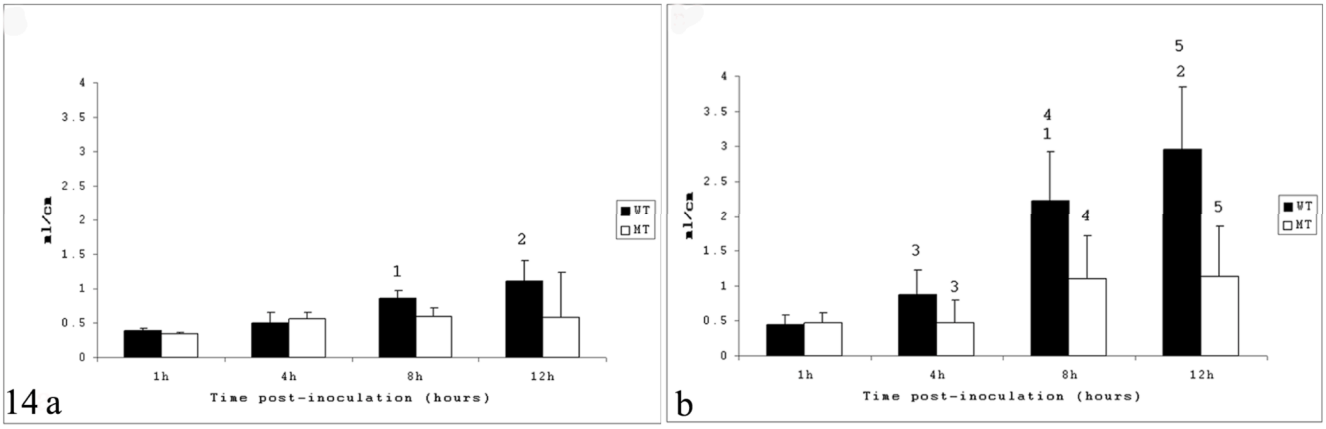


**Figure 14.**

Fluid accumulation in intestinal loops of CD18− (A) and CD18+ calves (B) infected with wild-type (WT) or mutant (MT) *Salmonella* Typhimurium and measured at 1, 4, 8, and 12 hours postinfection. Conditions labeled with the same number are statistically different ($P < .05$). CD18−, bovine leukocyte adhesion deficiency; CD18+, no deficiency.

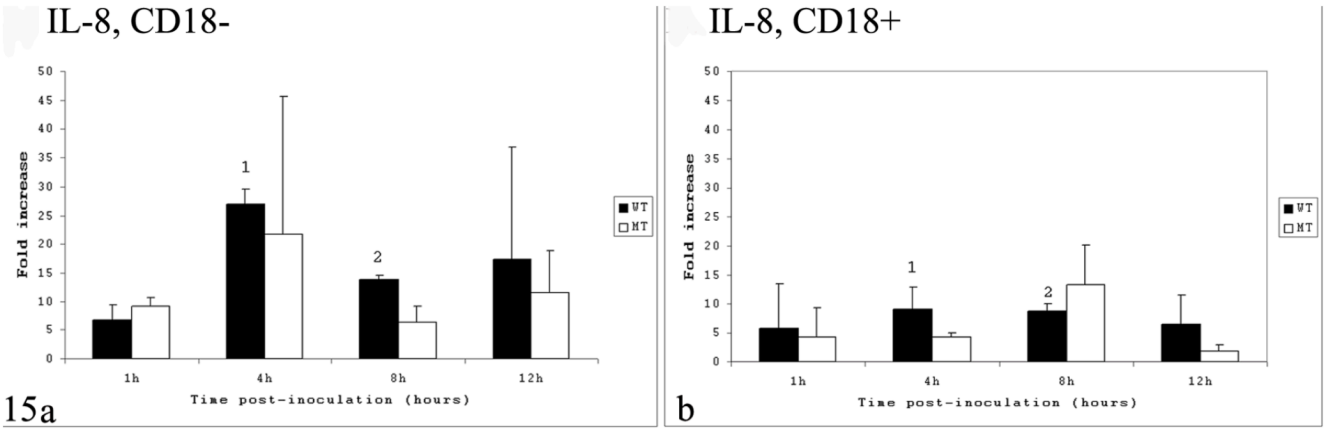


**Figure 15.**

Cytokine gene expression in intestinal loops of CD18− (A) and CD18+ calves (B), infected with wild-type (WT) or mutant (MT) *Salmonella* Typhimurium and measured at 1, 4, 8, and 12 hours postinfection. Gene expression of interleukin 8. Conditions labeled with the same number are statistically different ($P < .05$). CD18−, bovine leukocyte adhesion deficiency; CD18+, no deficiency.

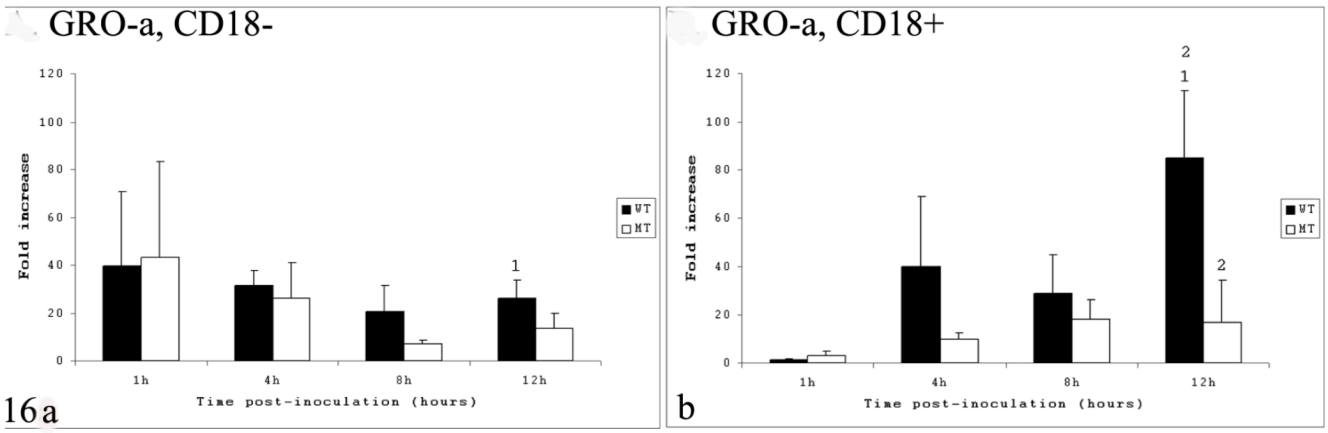


**Figure 16.**

Cytokine gene expression in intestinal loops of CD18− (A) and CD18+ calves (B), infected with wild-type (WT) or mutant (MT) *Salmonella* Typhimurium and measured at 1, 4, 8, and 12 hours postinfection. Gene expression growth-related oncogene α. Conditions labeled with the same number are statistically different ($P < .05$). CD18−, bovine leukocyte adhesion deficiency; CD18+, no deficiency.

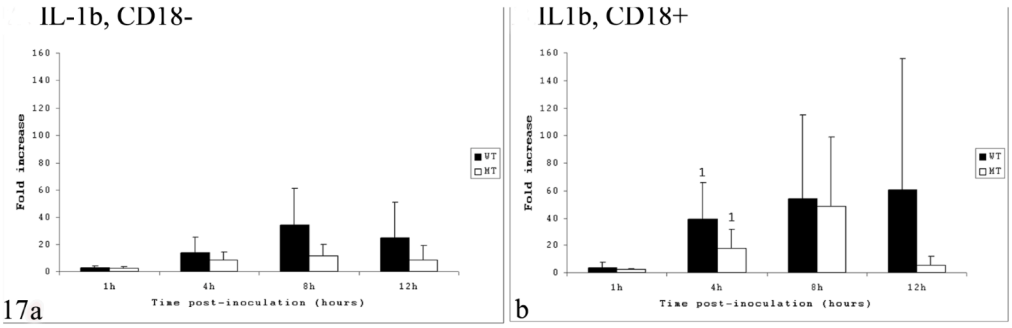


**Figure 17.**

Cytokine gene expression in intestinal loops of CD18− (A) and CD18+ calves (B), infected with wild-type (WT) or mutant (MT) *Salmonella* Typhimurium and measured at 1, 4, 8, and 12 hours postinfection. Gene expression of the proinflammatory cytokine interleukin 1β. Conditions labeled with the same number are statistically different ($P < .05$). CD18−, bovine leukocyte adhesion deficiency; CD18+, no deficiency.

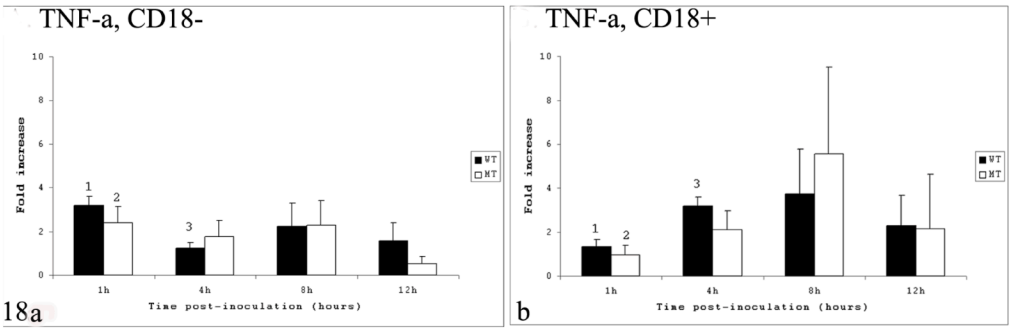


**Figure 18.**

Cytokine gene expression in intestinal loops of CD18− (A) and CD18+ calves (B), infected with wild-type (WT) or mutant (MT) *Salmonella* Typhimurium and measured at 1, 4, 8, and 12 hours postinfection. Gene expression of tumor necrosis factor α. Conditions labeled with the same number are statistically different ($P < .05$). CD18−, bovine leukocyte adhesion deficiency; CD18+, no deficiency.

## Table 1

Primer Sequences Used in Quantitative Real-Time Polymerase Chain Reaction to Study the Gene Expression of *Salmonella typhimurium*–Infected Bovine Intestine

| Target | Primer Sequence[a] | Amplicon Size (Base Pairs) |
|---|---|---|
| GAPDH | TTCTGGCAAAGTGGACATCGT<br>GCCTTGACTGTGCCGTTGA | 114 |
| GRO-α | CACTGCGACCAAACCGAAGT<br>GTATCAAGAAGCTCGTTCCAT | 153 |
| IL-8 | TGCTTTTTTGTTTTCGGTTTTTG<br>AACAGGCACTCGGGAATCCT | 71 |
| IL-1β | CCAGCCTGGCAAAAACCAT<br>CCGGAAATTGGTTCCACAGT | 201 |
| TNF-α | GTTCCTCACCCACACCATCAG<br>GGTAGTCCGGCAGGTTGATC | 283 |

[a]Sequences for bovine genes were obtained from GenBank. Top row represents forward primers and bottom row shows reverse primers. GAPDH, glyceraldehyde-3-phosphate dehydrogenase; GRO-α, growth-related oncogene α; IL-8, interleukin 8; IL-1β, interleukin 1β; TNF-α, tumor necrosis factor α. Figure 1–6